



ISTITUTO NAZIONALE DI FISICA NUCLEARE

Sezione di Milano

INFN/AE-02/02

20 Luglio 2002

HARP Note 02-004

**Construction of a Fast Laser-based Calibration System for the HARP
Tof counters wall**

M. Bonesini, M. Paganoni, A. Parravicini, A. Tonazzo

INFN – Sezione di Milano, Dip. di Fisica G. Occhialini, Pza. Scienza 3, Milano, Italy

A. Andreoni(*), M. Bondani(*), F. Paleari(*), A. Sottocornola-Spinelli

Dip. di Scienze Chimiche, Fisiche e Matematiche, via Voleggio 11, Como, Italy

(also at INFN, Sezione di Milano*

D. Gibin, A. Guglielmi, A. Menegolli

INFN – Sezione di Padova, Dip. di Fisica G. Galilei, via Marzolo 8, Padova, Italy

Abstract

A calibration and monitoring system for the Harp experiment scintillator-based time of flight system has been developed, by using an Nd-Yag laser with passive Q-switch and active/passive mode-locking and a custom made laser light injection system based on a bundle of IR monomode optical fibers. For the laser pulse timing a novel ultrafast InGaAs MSM photodiode, with 30 ps risetime, has been used. Experience over a several months data taking period in 2001 and 2002 shows that drifts in timing down to about 70 ps can be traced.

PACS:29.40.Mc

*Published by SIS-Pubblicazioni
Laboratori Nazionali di Frascati*

1 Introduction

The HARP experiment [1], shown in figure 1, has been constructed at CERN, on the PS T9 beamline, to study hadron production on nuclear targets for beam momenta between 2 and 15 GeV/c. The HARP spectrometer comprises about 15 different subdetectors to allow track reconstruction and particle identification over the full solid angle. In the forward direction, particle identification is performed at low momenta ($p \leq 3.5$ GeV/c) by a scintillator based TOF wall and at high momenta by a threshold Cerenkov counter.

The requirements for the forward TOF wall include excellent timing resolution, for particle identification, and good transverse segmentation to avoid particle pile-up on single counters. The system specifications called for a time resolution of $\sigma \simeq 250$ ps to separate at 4σ pions from protons up to 3.5 GeV/c, on the basis of a 10 m flight path. Particle identification is achieved combining leading-edge time measurements (from TDC) with pulse-height informations for time-walk corrections (from ADC). The mechanical structure of the HARP Tof wall is shown in figure 2. In the Left/Right palizades, scintillators are 250 cm long and lie vertically, while in the central palizade scintillators are 180 cm long and lie horizontally. The single scintillator counters are BC-408 bars from Bicron (see table I for details), 2.5 cm thick and 21 cm wide [2]. Each counter is read at the two extremes by a XP2020 photomultiplier (see table II for details). The analog signal is then fed, after a 40m long RG-213 cable ¹, to an active splitter chain in the counting room, that divides the signal 25% to the ADC line ² and 100% to the TDC line ³, after a leading edge discriminator,⁴.

For a particle crossing at a time t_0 a scintillator bar (equipped with two photomultipliers (PMT) i at the edges) at a distance x from its center, the time difference Δt_i between the STOP from the PMT i and the START from a reference counter t_s is given by:

$$\Delta t_i = t_0 + \frac{L/2 \pm x}{v_{eff}} - t_s + \delta_i \quad i = 1, 2$$

where L is the scintillator length, v_{eff} the effective light velocity in the scintillator bar ($v_{eff}^{-1} \simeq 5.9$ ns/m) and δ_i include all delays (cables, PMT transit time, ...). The quantity $\Delta t_+ = \frac{\Delta t_1 + \Delta t_2}{2} = t_0 + \frac{L}{2 \cdot v_{eff}} - t_s$ is independent from the impact point x along the counter and allows to measure the time of flight, while the impact position x can be deduced from $\Delta t_- = \frac{\Delta t_1 - \Delta t_2}{2} = \frac{x}{v_{eff}}$.

¹used instead of standard RG-58 coaxial cables, to minimize signal distortion

²based on CAEN V792, 12 bits, 32 channels modules

³based on CAEN V775, 12 bits, 32 channels modules

⁴model Lecroy 4413, 16 channel

The PMT i resolution is given by $\sigma_i^2 = \sigma_{\Delta t_i}^2 - \sigma_{t_s}^2$, while the crossing time (t_0) resolution is given by $\sigma_0 = \frac{1}{2}\sqrt{\sigma_1^2 + \sigma_2^2}$ and is expected to be equivalent to the one calculated directly from the distribution of Δt_- .

In the case of the Harp ToF Wall, the start reference counter (TOFB before the target), on loan from the previous NA52 experiment [3], is made of a plane of BC404 scintillators ($10 \times 10 \text{ cm}^2$) of 1 cm thickness, divided into eight strips of width growing from 0.8 cm to 2.0 cm at the outer edge. Every scintillator strip is matched to a plexiglas lightguide and read, at both ends, by PMT's. The intrinsic resolution of the counter is around 75 ps.

Drifts in delays are to be included in the calibration constants δ_i , that must be equalized at the beginning of the data taking period (at time T_0), for all the counters. Laser based systems have been extensively used for the time calibration of fast scintillator based TOF detectors. Usually the initial time equalization is obtained through cosmic rays calibration, while the the time evolution is obtained via a laser system. Previous systems include the ones used for the $N - \bar{N}$ experiment at Grenoble [4], the MARK-III experiment at SLAC [5], the CLAS system at CEBAF [6] and the TOPAZ experiment at KEK [7]. In our system (see later for details) the intrinsic resolution of the scintillator counters of the TOF wall has been preliminary evaluated at around 160 ps and this puts severe constraints on the calibration system, especially on the laser monitoring system. Timing drifts have to be traced down at better than 100 ps.

2 Hardware structure of the laser calibration system

A layout of the laser calibration system of the Harp ToF wall is shown in figure 3. The laser light is beam splitted to a fast photodiode, that gives the start for the TDC system and is injected into a bundle of fibers that transmit the pulse to the different scintillator channels. Given the requirement to spot out time drifts of the TOF system at the level of 1-2 TDC counts, e.g. down to 70 ps, all elements of the system: laser source, optoelectronic fiber system, fast photodiode for TDC start, injection system into the single scintillator bars, had to be carefully chosen.

For the light source of the monitoring system we used a custom made Nd-Yag laser ⁵ with passive Q-switch, active/passive mode locking and 10 Hz repetition rate. The infrared (IR) emission (at $\lambda = 1064 \text{ nm}$) is converted into a second harmonic at 532 nm by a KD*P SHG crystal. The Q-switch, to obtain short and powerful laser pulses, is obtained via a dye. The used dye was Exciton Q-switch I from Kodak, diluted into a dicloro-ethane solvent. According to the manufacturer's specification the laser had an output pulse width

⁵modified SYLPO from Quanta Systems srl, Via Venezia Giulia 28, Milano, Italy

in the IR of ~ 60 ps (FWHM) and an average energy per pulse of ~ 6 mJ, with an energy stability of $\pm 5\%$ for 95% of shots. The laser pulse average energy has been checked with a pyroelectric device ⁶, confirming the manufacturer’s specifications.

The pulse width (and by consequence the sharpness of the leading edge) is an essential point for our system. So we checked the manufacturer’s specifications for various concentration of the dye solution. The IR laser pulse width, before KD*P second harmonic generation, was directly measured with an optical technique based on autocorrelation [8]. An ad-hoc made autocorrelator was used for this measurement and is shown schematically in figure 4. Beam splitting the IR laser light and using two different optical paths, before recombination in the dichroic crystal (a KD*P), where the second harmonic generation (SHG) takes place, is thus possible to measure the laser pulse width, by varying the distance between the second mirror (S1) and the total reflection prism (the mirror position in Fig. 5). The width of the laser pulse can be immediately deduced, taking into account the relation $t = d/c$, with d mirror position in cm and c light velocity in vacuum. A typical result of such measurements is shown in figure 5, giving (65.1 ± 2.5) ps (FWHM) for the laser pulse width, in good agreement with the manufacturer’s specification. In order to take full advantage of the high-speed nature of our laser source, the device for timing the light pulse (and so give the TDC start) must also be very fast. For this purpose we used a novel design InGaAs MSM photodetector ⁷ with 30 ps rise and fall time, a low dark current of ~ 100 pA, 0.2×0.2 mm² sensitive area and a good radiant sensitivity between 450 and 850 nm. To get the optimal time performance, proper circuit connection was made against high frequency characteristics using a very broadband (≥ 10 GHz) “bias tee” ⁸ to power the diode. Due to the wide area covered by the TOF wall ($\sim 2.5 \times 7$ m²) and the requirement to have the laser source out of the experimental area for easy handling during beam data taking periods, relatively long fibers (~ 15 m) had to be used to inject the laser light into the single scintillator counters of the TOF wall. Fibers had been grouped in a bundle with a common part (~ 1 m) at the laser light injection and a free part going to the single counters. At the free end of each fiber the laser signal is injected into a short (1m long) multimode fiber ⁹ that ends in a small prism glued at the center of each scintillator bar. The use of a multimode fiber (with a bigger numerical aperture: 0.22 in the present case, to be compared to 0.14 of the used monomode fibers) allows the injection of the laser light into the scintillator bar at a direction nearer to the PMT axis (after first light reflection), giving a calibration signal prompter and more

⁶model Gentec ED-200

⁷Hamamatsu G4176

⁸model 5550B from Picosecond Pulse Lab

⁹CERAM OPTEC UV 100/125

similar to the one from cosmic rays muons. Before the injection in the fiber bundle, the laser light is attenuated by a system of optical neutral filters¹⁰ (OD ~ 4.5) to make the scintillator signal (from laser light) similar to the one from a minimum ionizing particle (MIP) and the laser beam spot is enlarged (to about 5 mm diameter) by a system of lenses to reduce intensity disuniformities.

3 Tests for fiber choice

The choice of the type of optical fiber in the bundle, to deliver the laser pulse to the individual scintillator bars is a critical issue. Precise timing requires a minimum modification to the time characteristics of the fast injected laser pulse or more precisely that the leading edge of the pulse (on which discrimination is done) has a minimum jitter. This condition is clearly achieved if the FWHM of the laser pulse is small (~ 50 ps) and has a negligible increase (dispersion), after propagation along the fibers of the bundle. Standard multimode fibers have typical dispersion of 30 ps/m and are clearly out of question for transmission along fibers 10-15 meters long. On the contrary, monomode fibers have small dispersions (typically $\ll 1$ ps/m), but the injection of the laser light into a monomode fiber bundle is a quite delicate task. Launch condition is essential to control the effective bandwidth of the used fibers. As an example, as respect to multimode fiber cores of $\sim 50 - 200 \mu m$, monomode fibers in the green have core diameter of $\sim 2 - 3 \mu m$ and IR monomode fibers have core diameters of $\sim 10 \mu m$, to be compared with a laser spot diameter of some mm. To reduce injection problems, we used larger core diameter IR monomode fibers (Corning SMF-28, see table III for details), that for green light behave as a “limited number of modes” fiber. To select the chosen fiber and test its dispersion characteristics we used the setup of figure 6. The light from a GE 100-1064-VAN Time Bandwidth SESAM laser ($\lambda = 532$ nm, after second harmonic generation, 9 ps FWHM laser pulse) is beam splitted to a single-photon avalanche photodiode [9] that gives the START to a TAC/SCA unit, with a 1.98 ps/ch resolution¹¹. The pulse shape is measured with a single photon timing technique. An optical fiber can be inserted, between the avalanche photodiode and the injection optics, to measure the additional spread introduced. Assuming a gaussian response function for the laser pulse, from measurements with and without the fiber under test, dispersion measurements can be done.

Results for the chosen fiber and a sample of discarded ones are shown in figure 7 and table IV. From the tests results, Corning SMF-28 fibers were chosen for the fiber bundle.

¹⁰Solid Glass ND filters, from Ealing Electro-optics

¹¹model 2145 from Canberra Instruments

This bundle ¹² consist of 61 fibers (15 m long) cutted at one edge, peeled and encapsulated in an optical cement matrix and then polished at the free surface. The other edge, after about 1 m, is completely free and has individual SMA connectors. The uniformity of the amplitude response of each individual fiber has been monitored with a Centronics AEPX65 photodiode, giving a dispersion of $\sim 36\%$ for the full bundle and $\sim 16\%$ for the chosen fibers (42 out of 61) to monitor the TOF wall scintillator bars. In this way time-walk corrections between different scintillator bars are minimized. As the precision of the individual fiber cutting length is around 10 cm, also the the time delay of each fiber had to be measured individually with two fast photodiodes¹³ and a large bandwidth oscilloscope. This additional delay has been accounted for in the following.

4 Performances of the laser calibration system

The laser calibration system, previously described, has been installed at the Harp experiment in May 2001 and has operated continuously between end July 2001 and beginning November 2001, during the experiment 2001 data taking and then from May 2002 onwards. The laser flash could be triggered externally, in the inter-spill, by a NIM level sent by a calibration trigger and so data could be accumulated in dedicated runs or during the standard data-taking . For each PMT channel, data consists of an ADC pulse-height Q_i and a TDC information Δt_i . Timing calibration of the TOF Wall system requires, in addition to ADC pedestals, the determination of the time-walk correction functions $f_i(Q)$ and relative time-offsets δ_i for each counter.

4.1 Tests of individual counters

4.1.1 Measurement of single counter timing resolution

The timing resolution for a scintillator counter read via PMT's, when illuminated by a light source (laser light or scintillator light) can be expressed by[10]:

$$\sigma = \sigma(N_{ph}, t_s, N_e, \sigma_{PMT}, \sigma_{elect})$$

where N_{ph} is the number of injected photons from the light source, t_s the light source characteristic time (laser pulse width or scintillator light decay time), N_e the photoelectrons number, σ_{PMT} the PMT time resolution and σ_{elect} the time resolution of electronics.

The time resolution of the Tof Wall counters has been measured both with dedicated cosmic rays runs, using a dedicated test bench during the construction, and with the laser

¹²bundle assembly from Fiberlan srl, Milano

¹³Hamamatsu G4176

system in situ. The laser light is injected into the center of each scintillator slab and the time recorded in both PMT. Time walk corrections (see later) are applied and ADC signals with averages compatible with a MIP are selected. However, some care has to be taken in the comparisons, due to the different mechanisms involved in the light generation. The time resolution can be evaluated plotting the quantity Δt_- for each slab, with dedicated laser runs. As an example, figure 8 shows the quantity Δt_- for the slab no. 15 (L= 250 cm) and the slab no. 2 (L= 180 cm), for a typical laser run. The obtained average intrinsic resolutions, as determined with the laser system, for all the Tof Wall counters are:

$$\sigma_L(L = 250 \text{ cm}) = 143 \pm 31 \text{ ps}$$

$$\sigma_L(L = 180 \text{ cm}) = 126 \pm 26 \text{ ps}$$

to be compared with:

$$\sigma_{CR}(L = 250 \text{ cm}) = 165 \pm 15 \text{ ps}$$

$$\sigma_{CR}(L = 180 \text{ cm}) = 145 \pm 14 \text{ ps}$$

as obtained from the cosmic rays runs, selecting events impinging at the center of each slab. The method used with the laser eliminates all contributions to timing resolution, which are common to both PMT's, including any jitter in the photodiode reference time.

4.2 System performance

4.2.1 Time-walk correction

The time-walk corrections were determined both with cosmic rays and laser data. In the same ADC range results are in agreement. Using additional neutral density filters to vary the laser light injected into the fiber bundle, the pulse-height Q_i and time differences Δt_i between a START (from the fast pin photodiode) and a common STOP (from the PMT scintillator) were recorded for different laser intensities. Figure 9 shows for a typical PMT channel the profile histogram of TDC Δt in ns vs the ADC pulse height Q in pC . The behaviour of each individual channel was parametrized with an exponential + low order polynomial function $f(Q)$, obtaining fit parameters for each individual channel.

4.2.2 Comparison with the cosmic rays calibration

The TOF WALL was calibrated at regular intervals, about every month or two during PS MD periods, with cosmic rays muons. The calibration procedure is quite lengthy (about 3 days of data taking) and so cannot be performed more frequently. These calibrations are used to determine the initial values of the equalization constants δ_i at time T_0 and to

make periodic recalibrations. The reliability of the time monitoring performed with the laser system was checked by comparing the variation of the time equalization constants δ_i obtained with cosmic rays calibration runs and laser calibration runs ($\Delta\delta_{CR}$ vs $\Delta\delta_{Laser}$). Results from this comparison are shown in Figure 10, that shows that differences are well within a ± 100 ps band. Figure 10 (a) shows differences at the beginning and the end of the August 2001 data taking, while Figure 10(b) shows the same differences between the 2002 data taking startup (May 2002) and the end of the 2001 data taking period (November 2001). Major interventions on the Tof Wall system were done in May 2002, resulting in changes of the time calibration constants δ_i up to ± 0.5 ns, as measured with cosmic rays. This change was well followed by the laser system, as shown by the previous plots. The rms of the difference between $\Delta\delta_{CR}$ and $\Delta\delta_L$ is around 70 ps. We can quote a total systematic error on the difference on calibration constants from two cosmic rays runs around 20 ps, due to various effects including the fit procedure, the different acceptance for MIP of the Tof wall counters, the time walk correction ... As a consequence we can safely apply a correction from laser data (at 1σ level) in presence of variation in timings of the counters bigger than ~ 60 ps.

4.2.3 Tof Wall time stability

The laser system can monitor the Tof wall stability daily over all the data taking period. As an example, before the 2001 data taking startup, one TDC modules (32 channels) had a shift of 5 counts (~ 175 ps), that was immediately spot out with the laser system and fixed. The TDC time differences $\Delta t_i(T)$, measured at time T of the data taking period and corrected for time walk, have been studied for all PMT channels i ($i = 1, \dots, 78$) to monitor the long term stability of the system. There is no evidence for time drift in excess of ~ 100 ps over the full 2001 data taking period (3 months long). Figure 11 shows the behaviour for two typical channels, as a function of the running time T. The distribution of the rms $\sigma_{\Delta t}$ for the individual channels of the TOF Wall, monitored after the full 2001 data taking period are shown instead in Figure 12. Possible drifts in the calibration constants δ_i of the TOF Wall system due to temperature effects on a night-day timescale have been studied. No clear effects are seen, showing that the TOF Wall system is stable within the limits shown before.

4.2.4 Tof Wall performance for particle identification

Particle identification in the HARP Tof Wall relies on the combination of particle momenta, as measured from the forward drift chambers and the time of flight between a start signal (t_s) from a reference counter before the target (TOFB) and a stop signal from the

Tof Wall itself. The previous calibration issues are essential for the quality of the extracted TOF PID and thus the determination of particle masses. After the calibration procedure, π and p are separated at better than 5σ at 3 GeV/c incident momentum.

5 Conclusions

A fast-laser based calibration system has been developed for the time calibration and monitoring of a large TOF counters wall for the Harp experiment. The intrinsic Tof Wall resolution of ~ 160 ps has put severe requirements on the calibration system. Time drifts down to about 70 ps can be monitored on a day by day timescale.

Acknowledgements

We thank Prof. A. Pullia and Prof. F. Bobisut for many discussions and the great help in the design of the presented calibration system. We are greatly indebted to Ing. C. Arnaboldi and Mr. F. Chignoli, R. Mazza of INFN Milano and Mr. G. Barichello and P. Gesuato of INFN Padua for technical help in system preparation. We acknowledge also the contribution of Dr. M. Tagliaferri of Quanta Systems srl for the laser construction at the best of our specifications and Dr. D. Batani of INFN Milano for the generous help in many tests.

density $\rho(g/cm^3)$	1.032
refractive index n	1.58
light yield (% of anthracene)	64
max emission $\lambda(nm)$	425
decay constant (ns)	2.1
bulk att. length (cm)	380

Table 1: Characteristics of the used BC408 scintillator from Bicron.

photocathode type	bialkali
Q.E. at 401 nm	$\sim 26\%$
Spectral sensitivity at 401 nm	85 mA/W
Anode pulse risetime	1.5 ns
Transit time jitter	0.25 ns
typical gain at 2200 V	$\sim 3 \times 10^7$
no. of dynodes	12

Table 2: Characteristics of the used XP2020 photomultipliers

core diameter	$8.2 \mu m$
NA	0.14
zero dispersion wavelength (λ_0)	1312 nm
zero dispersion slope (S_0)	$0.090 ps/(nm \times km)$
dispersion $D(\lambda)$	$\frac{S_0}{4}[\lambda - \frac{\lambda_0^4}{\lambda^3}]ps/(nm \times km)$ for $1200 nm \leq \lambda \leq 1600 nm$
refractive index difference	0.36%

Table 3: Characteristics of the IR monomode Corning SMF-28 fibers

fiber type	$\delta t/L$ (ps/m)	L (m)
FOS SMR-R (step index, single mode)	3.5	12 m
Ceram Optec UV 100/110 (multimode)	14.9	5.9 m
Corning SMF-28 (IR monomode)	3.6	15 m
Suhner FiberOptic 50/125	8.74	5.2 m

Table 4: Results of the tests of different multimode or monomode fibers as dispersion in ps/m

References

- [1] M.G. Catanesi et al., “Proposal to study hadron production for the neutrino factory and for the atmospheric neutrino flux”, CERN-SPSC/99-35, SPSC/P315, 15 November 1999
M.G. Catanesi et al., “Status report of the HARP experiment”, CERN-SPSC/2001-031, SPSC/M672, 29 October 2001.
- [2] G. Barichello et al., INFN/AE-02/01, 28 June 2002.
- [3] K. Pretzl et al., Invited talk at the “International Symposium on Strangeness and Quark Matter”, Kreete, 1999, p. 230.
- [4] M. Baldo Ceolin et al., *Nuovo Cimento* **105A** (1992), 1679
- [5] J.S. Brown et al., *Nucl. Instr. Meth.* **221** (1984) 503
- [6] E.S. Smith et al., *Nucl. Instr. Meth.* **A432** (1999) 265
- [7] T. Kishida et al., *Nucl. Instr. Meth.* **A254** (1987) 367
- [8] F. Zernike, *J. Midwinter Applied Nonlinear Optics*, J. Wiley, 1973
- [9] A. Sottocornola-Spinelli et al., *IEEE J. Quantum Electronics* **34** (1998), 817.
- [10] P. Benetti, M. Genoni, A. Tommaselli, *Nucl. Instr. Meth.* **A270** (1988), 411.

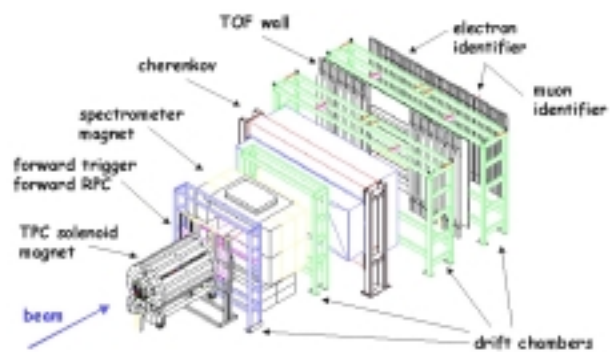


Figure 1: Layout of the Harp experiment at the Cern PS. The different sub-detectors are shown. The target is inserted inside the TPC. TOFB is at about 2.7 m before the target station.

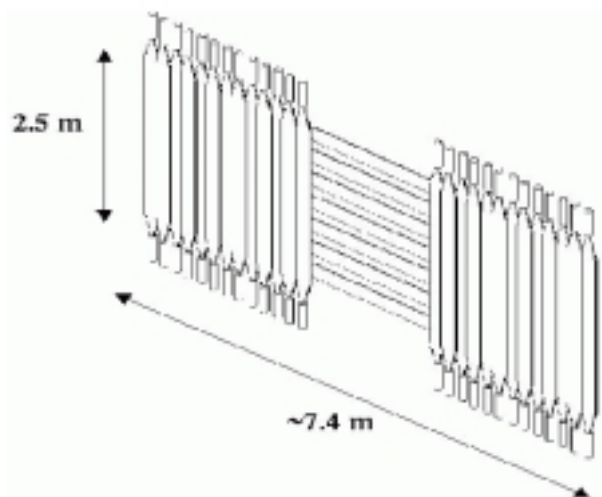


Figure 2: Layout of the TOF wall of the Harp experiment

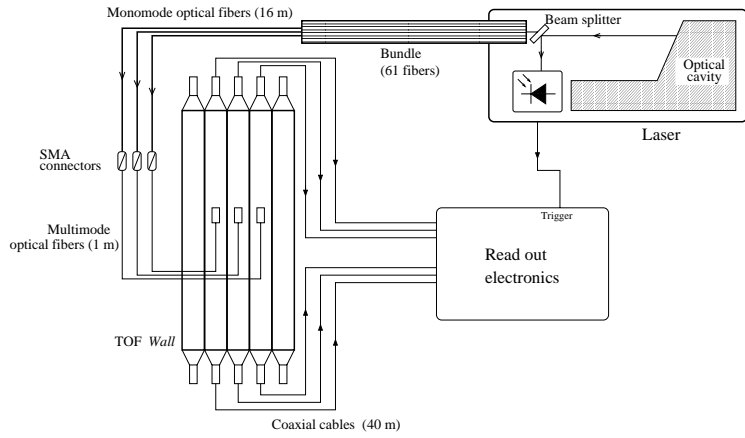


Figure 3: Layout of the laser calibration system for the Harp ToF Wall. For details on the single elements see text.

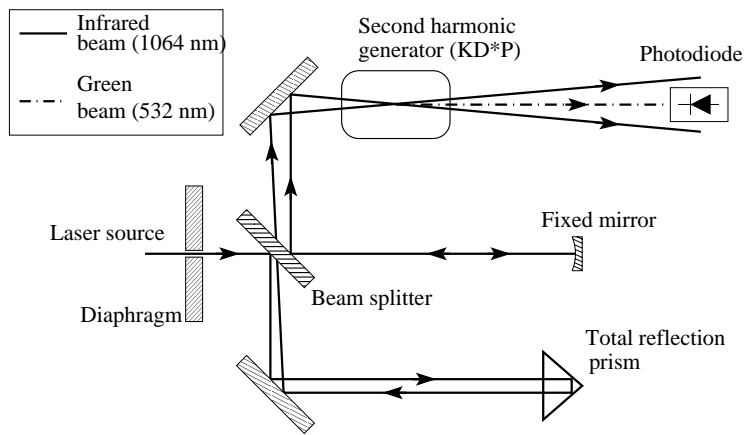


Figure 4: Layout of the autocorrelator setup, to test the laser pulse width.

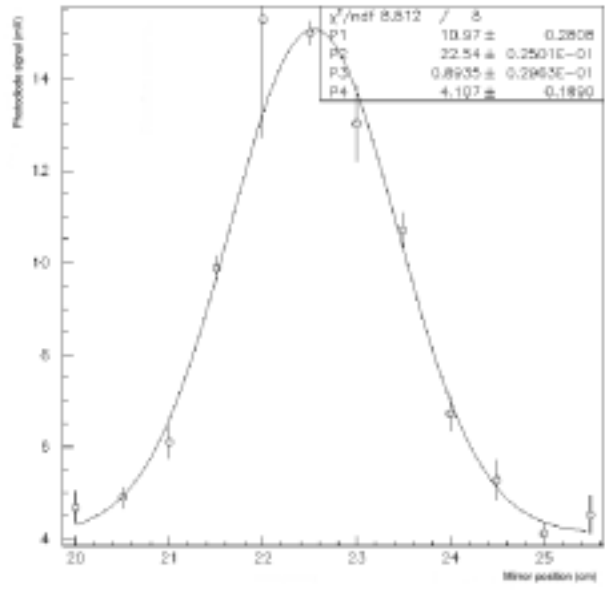


Figure 5: Result of a typical measurement for the width of the laser pulse, with the auto-correlator setup

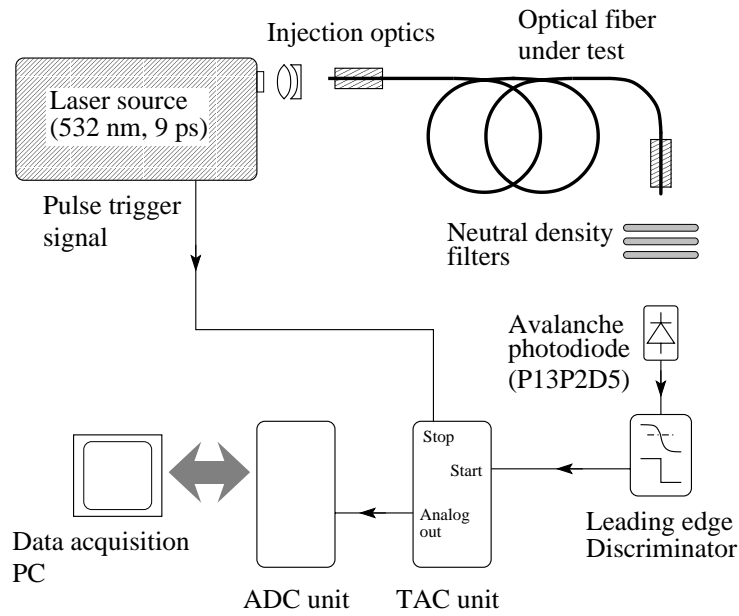


Figure 6: Layout of the fiber test setup, to study optical fiber dispersion characteristics

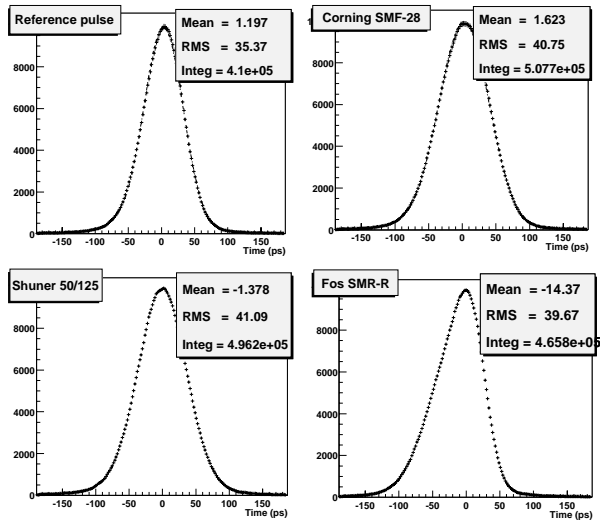


Figure 7: Shape of the laser pulse as measured at the end of different fiber types (b) (L=15 m), (c) (L=5.2 m), (d) (L=12 m), to be compared with the input laser pulse shape (a).

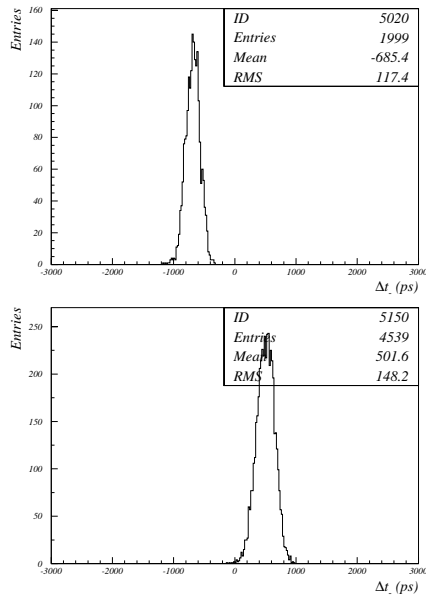


Figure 8: Δt_- distributions for a long (L= 250 cm) scintillator slab (upper) and a short (L= 180 cm) scintillator slab (lower), as measured with the laser system. No corrections are applied for the different channel delays.

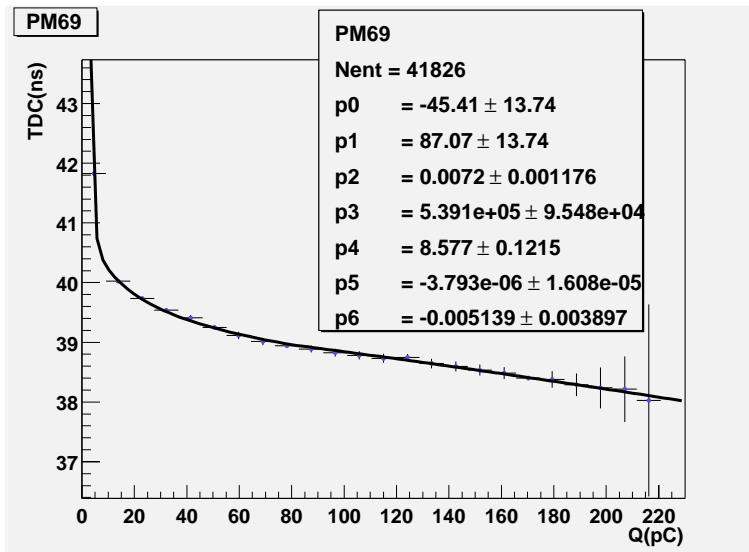


Figure 9: Dependence of the TDC times (ns) vs pulse height Q (ps) recorded in the QDC, for a typical PMT channel (no. 69). The fitted time-walk correction function $f(Q)$ is also shown.

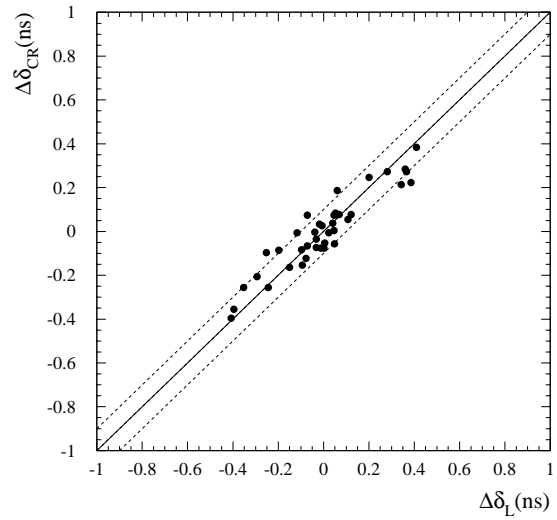
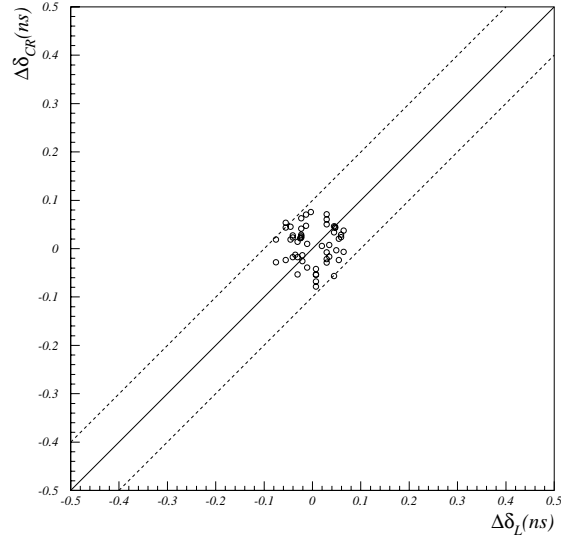


Figure 10: $\Delta\delta_{CR}$ are the drifts in the delay constants of each channel as measured with incoming cosmic ray muons at the beginning and the end of the 2001 August data taking period (a) and between May 2002 and November 2001 (b). $\Delta\delta_L$ are the same drifts as measured with the laser system. The width of the dotted band in the plots is ± 70 ps. The rms of the differences of $\Delta\delta_{CR}$ and $\Delta\delta_L$ are less than ± 70 ps.

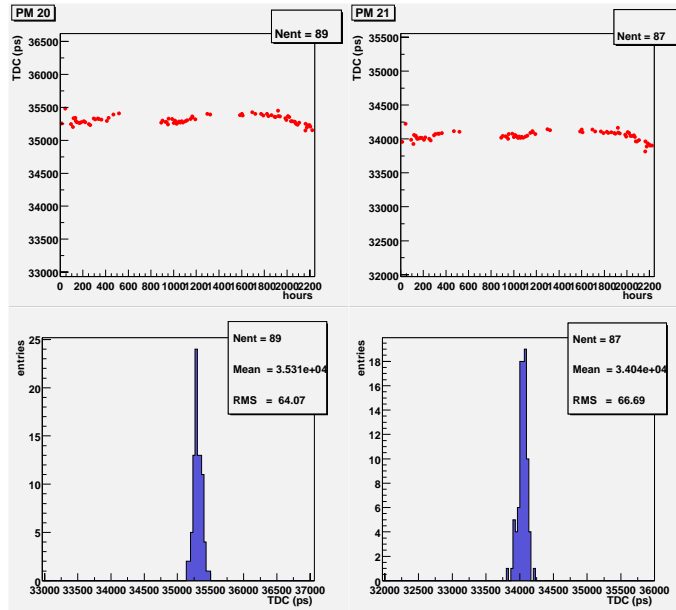


Figure 11: Variation of Δt vs running time T (2001 data taking: 3 months) for two typical PMT channels.

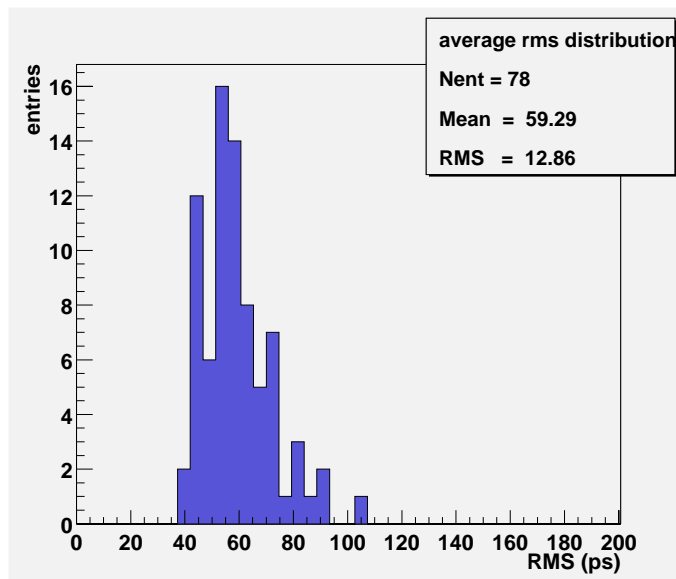


Figure 12: Histogram of the rms $\sigma_{\Delta t}$ for all the TOF Wall PMT channels, monitored over the full 2001 data taking period.